THE JOURNAL OF BIOLOGICAL CHEMISTRY
Vol. 279, No. 10, Issue of March 5, pp. 9481–9489, 2004
Printed in U.S.A.
© 2004 by The American Society for Biochemistry and Molecular Biology, Inc.

Glycosylphosphatidylinositol-anchored Proteins and Actin Cytoskeleton Modulate Chloride Transport by Channels Formed by the *Helicobacter pylori* Vacuolating Cytotoxin VacA in HeLa Cells*[S]

Received for publication, November 3, 2003, and in revised form, December 11, 2003
Published, JBC Papers in Press, December 14, 2003, DOI 10.1074/jbc.M312040200

Nils C. Gauthier‡§, Vittorio Ricci¶, Pierre Gounon‖, Anne Doye‡, Michel Tauc, Philippe Poujeol**, and Patrice Boquet‡ ‡‡**

*From ‡INSERM U 452, IFR 50, Faculté de Médecine 28 Avenue de Valombrose, 06107 Nice, France, the ¶Department of Experimental Medicine, Human Physiology Section, University of Pavia, 27100 Pavia, Italy, the ‖Centre Commun de Microscopie Appliquée, Université de Nice, 06108 Nice, France, and **CNRS UMR 65-48, Faculté des Sciences, Parc Valrose, 06108 Nice, France*

The vacuolating cytotoxin VacA is an important virulence factor of *Helicobacter pylori*. Removing glycosylphosphatidylinositol-anchored proteins (GPI-Ps) from the cell surface by phosphatidylinositol-phospholipase C or disrupting the cell actin cytoskeleton by cytochalasin D reduced VacA-induced vacuolation of cells (Ricci V., Galmiche, A., Doye, A., Necchi, V., Solcia, E., and Boquet, P. (2000) *Mol. Biol. Cell* 11, 3897–3909). Using the fluorescent dye 6-methoxy-*N*-ethylquinolinium chloride, an indicator for cytosolic chloride, we have investigated the role of either GPI-Ps or actin cytoskeleton in the activity of the selective anionic channel formed by VacA at the plasma membrane level. Removal of GPI-Ps from HeLa cell surfaces did not impair VacA localization into lipid rafts but strongly reduced VacA channel-mediated cell influx and efflux of chloride. Disruption of the actin cytoskeleton of HeLa cells by cytochalasin D did not affect VacA localization in lipid rafts but blocked VacA cell internalization and inhibited cell vacuolation while increasing the overall chloride transport by the toxin channel at the cell surface. Specific enlargement of Rab7-positive compartments induced by VacA could be mimicked by the weak base chloroquine alone, and the vacuolating activities of either chloroquine alone or VacA were blocked with the same potency by the anion channel blocker 5-nitro-2-(3-phenylpropylamino)-benzoic acid shown to inhibit VacA channel activity (Tombola, F., Oregna, F., Brutsche, S., Szabò, I., Del Giudice, G., Rappuoli, R., Montecucco, C., Papini, E., and Zoratti, M. (1999) *FEBS Lett.* 460, 221–225). We suggest that formation of functional VacA channels at the cell surface required GPI-Ps and that endocytosis of these channels by an actin-dependent process increases the chloride content of late endosomes that accumulate weak bases, provoking their enlargement by osmotic swelling.

The VacA cytotoxin (1, 2) is an important pathogenic determinant involved in *Helicobacter pylori* bacterial colonization (3). VacA is a single chain protein (molecular mass, 90 kDa) that contains N-terminal (p34; molecular mass, 34 kDa) and C-terminal (p58; molecular mass, 58 kDa) polypeptide domains (4). The purified cytotoxin forms hexamers or heptamers (5, 6) that can assemble into dodecamers (5). Cells such as HeLa incubated with monomeric VacA (but not with the oligomeric form of the toxin) in the presence of weak bases such as NH_4Cl, developed large Rab7-positive intracellular vacuoles (*i.e.* late endosomes) (7). Purified VacA must be "activated" by a rapid acid or alkaline treatment to render it monomeric (2). VacA-induced vacuolation strictly requires an active V-ATPase on the endosomal membrane to allow vesicular acidification (2).

Oligomerized VacA monomers form anion-selective channels in artificial lipid membranes (8–11). The presence of similar anionic channels formed by VacA was then detected at the level of the plasma membrane of HeLa cells and found only when the toxin was activated (11, 12). There is evidence that links the formation of VacA anionic channel to the toxin-induced vacuolation (2). However, it is not clear where the VacA channel is formed in the cell because vacuolation can be induced by intracellular expression of the toxin (2). The toxin may assemble a channel directly at the cell surface (12) or, after endocytosis and translocation into the cytosol, may form a pore in the limiting membrane of intracellular compartments such as late endosomes (13, 14). The notion that VacA channel structure and activity observed in artificial lipid bilayers (8–11) might be similar to those found in living cells (11, 12) has been also challenged recently (15). For instance, both the number of toxin oligomers and the characteristics of the molecular ultrastructure of the VacA channel were found to be different from those observed in artificial lipid bilayers (15).

VacA is endocytosed by cells (16–18) via a clathrin-independent pathway (18). Treatment of highly sensitive cells to VacA with PI-PLC,[1] which specifically removes proteins anchored to the plasma membrane via a GPI link (19), reduced and delayed VacA-induced cell vacuolation (17, 18). It has been furthermore reported that although GPI-Ps were not apparently required directly for the binding of VacA to cells (17, 20), the toxin may exploit the GPI-Ps pathway of endocytosis (17). Although GPI-Ps appear to freely diffuse throughout the cell plasma membrane, they may reside preferentially in detergent-resistant membrane domains (named lipid rafts (21)) (22) and, in

* This work was supported by INSERM (Paris, France). The costs of publication of this article were defrayed in part by the payment of page charges. This article must therefore be hereby marked "*advertisement*" in accordance with 18 U.S.C. Section 1734 solely to indicate this fact.

[S] The on-line version of this article (available at http://www.jbc.org) contains supplemental videos.

§ Submitted in partial fulfillment of the requirements for a Ph.D. degree (Université de Nice Sophia-Antipolis, France). Supported by a Ph.D. grant from the Ministère de la Recherche et de la Technologie.

‡‡ To whom correspondence should be addressed. Tel.: 33-4-9353-1755; Fax: 33-4-9353-3509; E-mail: boquet@unice.fr.

[1] The abbreviations used are: PI-PLC, phosphatidylinositol-phospholipase C; GPI-P, glycosylphosphatidylinositol-anchored protein; CD, cytochalasin D; NPPB, 5-nitro-2-(3-phenylpropylamino)-benzoic acid; MEQ, 6-methoxy-*N*-ethylquinolinium; GFP, green fluorescent protein; mAb, monoclonal antibody; HBSS, Hanks' balanced salt solution; NM, NaCl medium; GM, gluconate medium; CHO, Chinese hamster ovary.

Downloaded from http://www.jbc.org/ by guest on July 27, 2018

certain cases, be endocytosed via a clathrin-independent pathway (23). In addition, treatment of cells with the cholesterol-sequestering drug nystatin or β-methylcyclodextrin, known to disrupt lipid rafts, strongly impaired VacA activity (18, 20, 24). This indicated that lipid rafts are involved in the molecular mechanism of VacA-induced vacuolation. Accordingly, it has been shown that VacA is associated with lipid rafts (20, 24).

The actin cytoskeleton appears also to play an important role in VacA-induced vacuolation. It was first reported that conditional expression of dominant positive or negative mutant forms of Rho GTPases, well known regulators of F-actin structures organization, were able to modulate the vacuolation induced by VacA (25). Then it was shown that disruption of the actin cytoskeleton by CD was able to decrease the toxin-induced vacuolation of HEp-2 cells without impairing the intracellular activity by which VacA provokes the formation of large vacuoles (18).

In the present work we have examined the effects of the removal of GPI-Ps from the cell surface or the disruption of the actin cytoskeleton, treatments both known to reduce VacA-induced vacuolation (18), on the activity of the anion-selective channel formed by the toxin in HeLa cells. We have shown that GPI-Ps are lipid raft components required for the formation of active or fully functional VacA channels at the level of the cell surface but not for the cell binding of the toxin. In contrast, disruption of the actin cytoskeleton of HeLa cells did not interfere with the VacA pore transport of chloride ions and even increased its anion channel function. Finally, we have shown that specific swelling of Rab7-positive compartment, a characteristic feature of VacA (2), could also be achieved with low concentrations of the weak base chloroquine alone and that the anion channel blocker NPPB inhibited not only the VacA-induced vacuolation but also the chloroquine-induced vacuolation.

EXPERIMENTAL PROCEDURES

Cell Line, Transfection, Bacterial Strain, VacA Toxin, and Antibodies—HeLa cells (human cervix carcinoma), a gift form Dr. T. L. Cover (Vanderbilt University, Nashville, TN), were cultured and transfected as previously described (18). The cells were transfected with eukaryotic vectors allowing the expression of proteins fused to the green fluorescent protein (GFP), namely: GFP-Rab 7, a fusion at the N terminus of Rab 7 with GFP; and GFP-Rab 5, also a fusion at the N terminus of Rab 5 with GFP. These constructs were kindly provided by Dr. A. Galmiche (INSERM U452, Nice, France).

The VacA-producing *H. pylori* 60190 strain (ATCC 49503, with a type s1a/m1 *vacA* genotype) was used to produced the cytotoxin. Purification of VacA was achieved according to Cover and Blaser (26). Immediately before use on cells, purified VacA was activated according to de Bernard *et al.* (27).

The anti-VacA rabbit polyclonal IgG 958 (16), kindly given by Dr. T. L. Cover (Vanderbilt University), was used throughout this work. The anti-CD55 was a rabbit polyclonal antibody (Santa Cruz Biotechnology, Santa Cruz, CA) directed against the GPI-P CD55 (28), whereas the mouse mAb anti-CD59 (29) was a gift from Dr. M. Deckert (INSERM U576, Nice, France). The mAb anti-flotillin-1 was from BD Biosciences (Le Pont de Claix, France). Secondary antibody against rabbit IgG labeled with Texas Red was from Molecular Probes (Eugene, OR). Anti-mouse IgG antibody labeled with fluorescein isothiocyanate as well as anti-rabbit and anti-mouse IgG antibodies conjugated with horseradish peroxidase were from Dako (A/S, Denmark). Phalloidin-fluorescein isothiocyanate was from Sigma-Aldrich.

Neutral Red Dye Uptake, Acridine Orange Assay, Time Lapse Imaging, PI-PLC, CD and NPPB Cell Treatments, Immunofluorescence, and Immunoblotting—The degree of cell vacuolation was quantified by means of neutral red dye uptake assay and was expressed as micrograms of neutral red/micrograms of cell protein (30). In experiments using chloroquine without VacA to induce cell vacuolation, after triple rinsing in HBSS cells were incubated for 5 h in HBSS containing 1 mM chloroquine. In experiments testing the effect of NPPB (Calbiochem, La Jolla, CA) on cell vacuolation, NPPB was added in HBSS-NH_4Cl or HBSS-chloroquine.

The pH-sensitive fluorescent dye acridine orange (Sigma-Aldrich) (5 μg/ml) was incubated with living cells for 10 min at room temperature in phosphate-buffered saline in the dark. After three washes in phosphate-buffered saline, the living cells where then directly observed by confocal microscopy (Leica TCS-SP, Heidelberg, Germany).

For time lapse imaging, the cells were filmed for 2 h in constant conditions of 5% CO_2 and 37 °C and observed by phase contrast optics using an Axiovert 200 microscope (Carl Zeiss, Göttingen, Germany) with shutter-controlled illumination (Carl Zeiss) and cooled digital CCD camera (Roper Scientific, Evry, France). The images were recorded at 1 frame/30 s and accelerated at 10 frames/s in the videos using Metamorph 2.0 image analysis software (Universal Imaging Corporation, Evry, France) and QuickTime pro 5 (Apple).

The treatments with PI-PLC and CD (Sigma-Aldrich) were performed as previously described (18), excepted that the incubation of cells with PI-PLC (in HBSS containing cycloheximide to prevent further synthesis of GPI-anchored proteins) was performed for 2 h at 37 °C. The anion channels blocker NPPB was added, after VacA intoxication, at the indicated concentrations. The immunofluorescence studies were performed as described previously (18). For immunoblotting, the proteins were resolved on 10% SDS-PAGE followed by transfer on nitrocellulose membranes (Amersham Biosciences).

Patch Clamp and MEQ Chloride Transport Assays—The whole cell patch clamp configuration was used. To control the absence of cystic fibrosis transmembrane conductance regulator channels in HeLa cells, 10 μM dibromo-AMPc (Sigma-Aldrich) plus 10 μM forskolin (Sigma-Aldrich) were used. Whole cell currents were monitored with an RK 400 amplifier (Biologic, Münster, Germany). In all experiments the membrane potential was clamped at −50 mV, and 400-ms pulses were applied in 20-mV steps from −100 to +80 mV, with 3-s intervals between pulses.

MEQ was synthesized in the laboratory and utilized according to Biwersi and Verkman (31). Changes in fluorescence were recorded with a CCD camera (Photonics Sci, Robertsbridge, UK). The results were analyzed using the Axon software (Axon Instruments, Union City, CA). For each experiment, fluorescence from microscopic fields, each containing an average of 8–24 cells, was recorded and quantified. The results are expressed as relative fluorescence F/F_0, where F is the fluorescence as a function of time, and F_0 is the minimum fluorescence recorded after fluorescence quenching with the final thiocyanate substitution (140 mM potassium thiocyanate, 3 mM calcium gluconate, 10 mM Hepes buffer, pH 7.4). The histograms represent the change rate of the fluorescence (absolute values) of three independent experiments during the substitutions with either NaCl medium (NM) or gluconate medium (GM). The osmolarity of all media was adjusted with mannitol to 340 milliosmoles.

Analysis of Lipid Rafts by Density Gradient—The cells (3×10^6) were plated in 100-mm tissue culture dishes 24 h before use. Activated VacA was added to cells for 1 h in HBSS at 4 °C. The cells were then washed and transferred into warmed HBSS (37 °C) for the indicated period of time. After triple rinsing with cold phosphate-buffered saline, the cells were scraped off the dishes in calcium-free phosphate-buffered saline and centrifuged ($1000 \times g$, 5 min, 4 °C). The cells were then lysed 30 min at 4 °C in TNE buffer (25 mM Tris-HCl, 150 mM NaCl, 5 mM EDTA) containing 1% Triton X-100 and a mix of protease inhibitors (Complete EDTA-free; Roche Applied Science). Optiprep 60 (Axis-Shield, Oslo, Norway) was added to the lysate at the bottom of an ultracentrifuge tube (Beckman, Palo Alto, CA) to obtain a 40% final concentration. A layer of Optiprep 30% (Optiprep 60 diluted in TNE) and a final layer of TNE were respectively added. After centrifugation ($100,000 \times g$, 2 h, 4 °C), eight fractions from the top to the bottom of the tube were collected and analyzed by immunoblotting. The immunoblots were scanned, and quantification of the signals was performed using the NIH Image 1.63 software.

Ultrastructural Studies and VacA Immunogold Labeling—HeLa cells treated with CD for 1 h and incubated with CD and acid-activated VacA (2 μg/ml) for 4 h at 37 °C were fixed with 2% (w/v) paraformaldehyde (Sigma-Aldrich) or with a mixture of 2% (w/v) paraformaldehyde and 0.2% (w/v) glutaraldehyde (Sigma-Aldrich) in 0.1 M phosphate buffer (pH 7.5) for 1 h. The cell pellets were washed with phosphate buffer, embedded in 10% (w/v) gelatin, and infused in 2.3 M sucrose. Mounted gelatin blocks were frozen in liquid nitrogen, and ultrathin sections were prepared with an ultracryomicrotome (Leica, Vienna, Austria). Ultrathin cryosections were collected with 2% (w/v) methylcellulose, 2.3 M sucrose, and immunogold-labeled with VacA antibodies and anti-rabbit IgG coupled to 10-nm gold particles.

Downloaded from http://www.jbc.org/ by guest on July 27, 2018

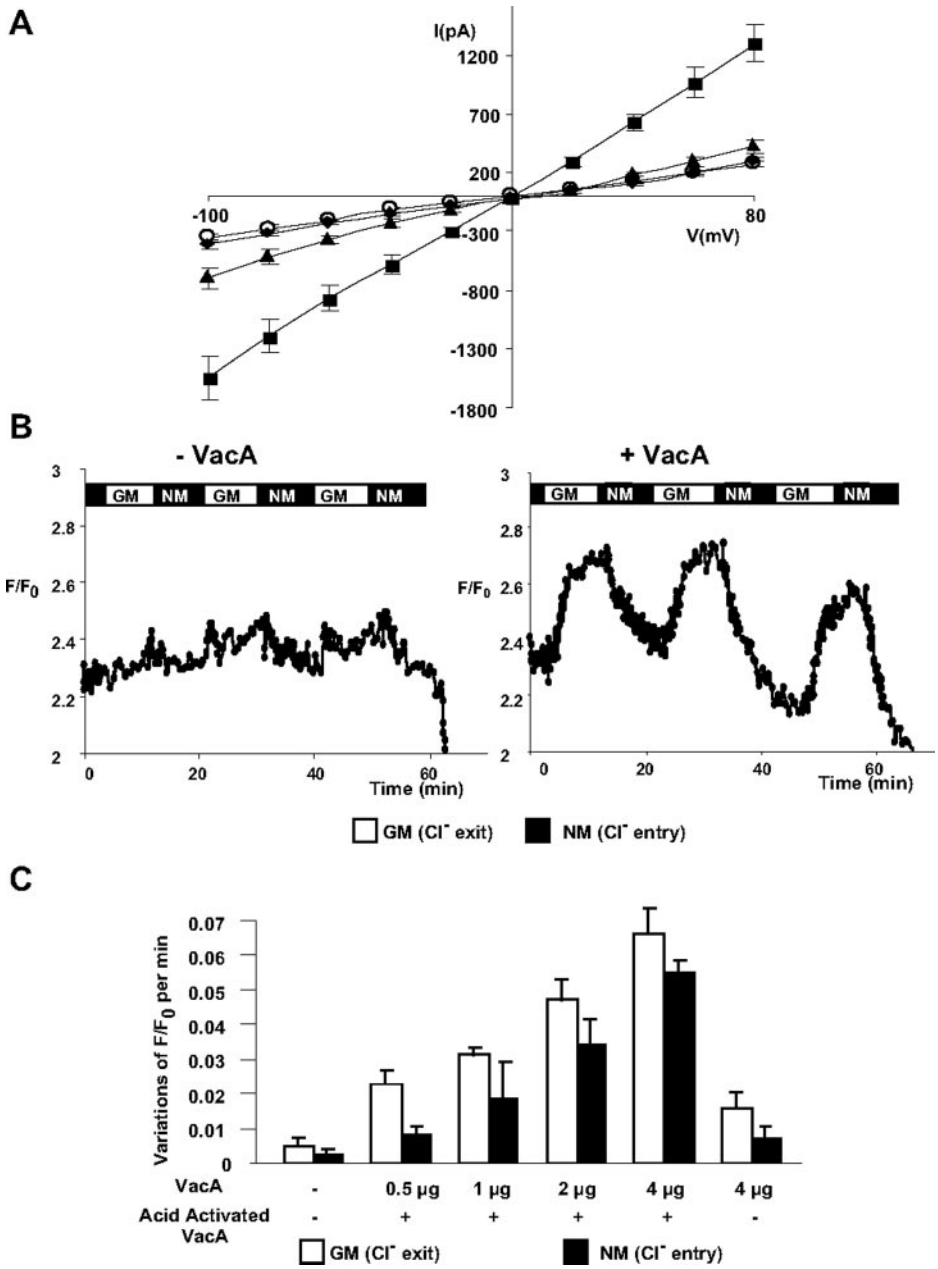

FIG. 1. **Assays by patch clamp or by the halide-sensitive fluorescent probe MEQ of the VacA channel inserted in the HeLa cell plasma membrane.** *A*, *I/V* plots of whole cell patch clamp recording from HeLa cells treated with VacA (2 μg/ml) during 30 min (■, $n = 8$), with VacA in the presence of 100 μM NPPB (▲, $n = 8$), without VacA intoxication (○, $n = 14$), or without VacA but in the presence of 10 μM dibromo-AMPc and 10 μM forskolin (◆, $n = 9$). *B*, HeLa cells were incubated or not with VacA (2 μg/ml) for 30 min at 37 °C and loaded with MEQ as described under "Experimental Procedures." Chloride-sensitive dye MEQ fluorescence was estimated by recording the fluorescence of microscopic fields (each containing an average of 16 cells) with a CCD camera upon sequential buffer substitution with GM followed by NM. The relative fluorescence (F/F_0) of MEQ was measured as a function of time. *C*, histograms representing variations of the relative MEQ fluorescence slopes (absolute values) during GM (*white columns*) or NM (*black columns*) substitutions of cells treated or not with VacA (0.5, 1, 2, and 4 μg/ml) or nonactivated VacA (4 μg/ml). Each histogram represents an average of three independent experiments with a recording of 8–24 cells in each assay.

RESULTS

The VacA Channel Activity, Inserted in the HeLa Cell Plasma Membrane, Can Be Tested by the Technique Using the Halide-sensitive Fluorescent Probe MEQ—Incubation of HeLa cells for 30 min at 37 °C with 2 μg/ml of acid-activated purified VacA induced a clear increase in the cell current studied by the whole cell patch clamp technique as described previously (11, 12) (Fig. 1*A*). The current was inhibited by the addition of 100 μM of the chloride channel blocker NPPB (Fig. 1*A*), indicating that VacA caused a chloride flux as previously reported (11, 12). Channel activity required toxin acid activation (not shown), and as reported (12), no interference with cystic fibrosis transmembrane conductance regulator channel in HeLa cells appeared to be possible because no current increase was detected after the addition of forskolin and dibromo-AMPc to the patched cell (Fig. 1*A*). Because the whole cell patch clamp technique does not allow observation of channels in a large number of cells for a long period of time or is cumbersome after various cell treatments (such as CD or PI-PLC), we decided to use the fluorescent dye MEQ, an indicator for cytosolic chloride (31). In aqueous buffers, the fluorescence of MEQ is quenched by Cl^-, thereby allowing a quantification of this ion in the cytosol (31). The cells were incubated with acid-activated VacA for 30 min at 37 °C, loaded with MEQ at 20 °C for 5 min, and tested at room temperature (20 °C) for the formation of chloride channels. Substitution of the NM by GM should lead to an increase of MEQ fluorescence (dequenching) if chloride channels are functional in the cell plasma membrane. A subsequent substitution by NM should induce an influx of Cl^- ions and thus a quenching of MEQ fluorescence. As shown in Fig. 1*B*, in the absence of VacA no modification of MEQ fluorescence was observed by 10-min substitutions by either GM or NM. When the cells were intoxicated with 2 μg/ml of acid-activated VacA, iterative substitutions by GM followed by subsequent additions of NM resulted in a series of increase and decrease in MEQ fluorescence (Fig. 1*B*). The MEQ fluorescence technique therefore allowed us to measure the presence of channels for chloride transport formed by the VacA toxin. VacA channels activity appeared to be stable for a long time without any significant decrease in the anion transport as expected if the toxin chan-

Downloaded from http://www.jbc.org/ by guest on July 27, 2018

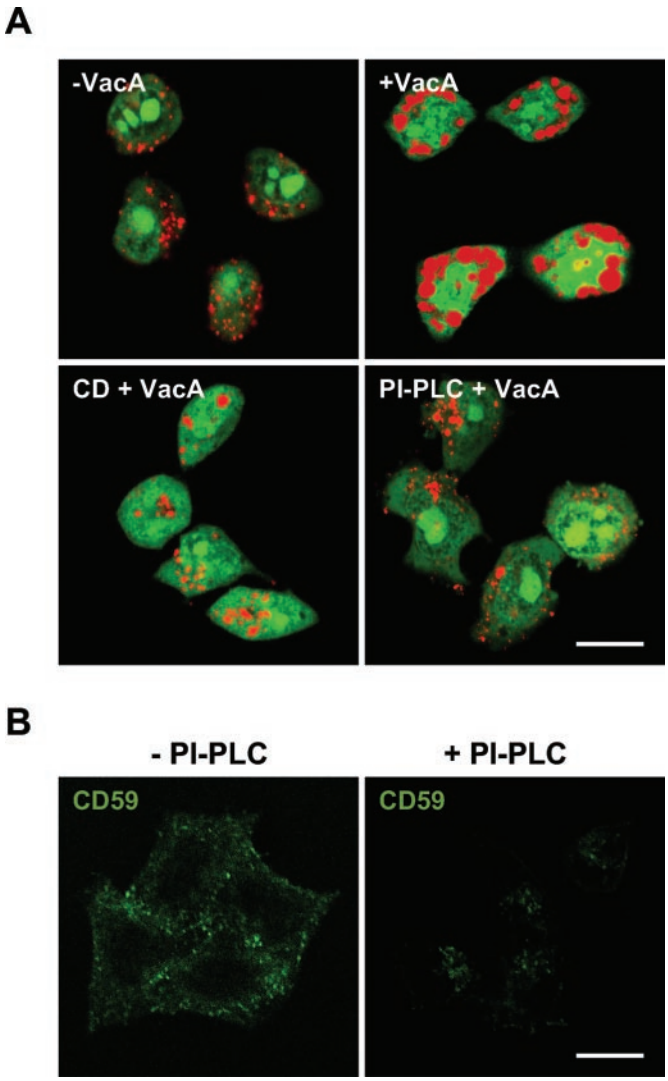

FIG. 2. **Removing GPI-Ps from cell surface or disrupting the F-actin cytoskeleton decreases HeLa cells VacA-induced vacuolation.** *A*, HeLa Cells grown on coverslips and treated or not with PI-PLC plus cycloheximide or CD were incubated with VacA (2 μg/ml) for 30 min at 37 °C excepted for control, then washed, and maintained for 4 h in HBSS with 5 mM NH_4Cl to allow the development of cell vacuolation. The living cells were stained with acridine orange (see "Experimental Procedures") (acridine orange displays a red fluorescence at acidic pH and a green fluorescence at neutral pH). The pictures represent one confocal section (representative for at least four independent experiments). *B*, control of PI-PLC treatment efficiency. The GPI-P CD59 was detected with a mouse monoclonal antibody followed by a polyclonal fluorescein isothiocyanate-coupled secondary antibody. Fluorescence analysis of confocal sections of cells not treated (*left picture*) or treated with PI-PLC (*right picture*) was performed with the same laser excitation intensity. *Scale bars*, 10 μm.

nels were endocytosed. This may be due to the fact that the MEQ assay was performed at 20 °C, a temperature at which there is a low activity of membrane internalization, thus possibly allowing toxin channels to stay at the cell surface. The chloride channel activity of VacA appeared concentration-dependent (Fig. 1*C*), and channel formation required the acid activation of the toxin (Fig. 1*C*).

Depolymerization of Actin Cytoskeleton of HeLa Cells by CD Blocks Toxin Endocytosis—We next examined whether PI-PLC and CD treatments were also effective in reducing the VacA-induced vacuolation in HeLa cells. For this purpose we used the pH-sensitive indicator acridine orange that accumulates and decorates the large vacuoles formed by VacA. As shown in Fig. 2*A*, incubation of HeLa cells with 2 μg/ml of VacA in the presence of 5 mM NH_4Cl for 4 h induced the formation of numerous, large, acidic vacuoles as compared with untreated preparation (Fig. 2*A*). Treatment of cells with PI-PLC before their incubation with VacA strongly reduced the formation of large vacuoles (Fig. 2*A*). The efficiency of PI-PLC treatment was controlled by the ability of this phospholipase to remove the GPI-P CD59 (29) (Fig. 2*B*).

As previously shown (18), depolymerization of the actin cytoskeleton by CD also blocked the formation of large acidic vacuoles in HeLa cells (Fig. 2*A*). We next investigated whether the entry of VacA was still occurring when cells were treated with the actin-depolymerizing agent CD. For that purpose we studied by indirect immunofluorescence and confocal microscopy the localization of the toxin incubated with HeLa cells for 1 h at 4 °C by the same procedure described by Garner and Cover (16). As shown in Fig. 3*A*, cells incubated with VacA (2 μg/ml) for 1 h at 4 °C, then washed, and incubated for 30 min at 37 °C internalized the toxin as evidenced by the presence of numerous toxin-containing vesicles. Our results were different from those of Garner and Cover (16) who found an accumulation of VacA into intracellular vacuoles only 4 h after the onset of toxin endocytosis. This may be due to the procedure of cell permeabilization used. Indeed, Garner and Cover (16) used methanol, whereas we utilized Triton X-100 for permeabilization. Vesicles containing VacA were clearly inside the cell because they were visualized only under permeabilized condition (Fig. 3*A*). When cells were treated with CD, before and during VacA incubation, the toxin was strictly co-localized at the level of the cell surface with large membrane protrusions formed by nonspecific polymerized patches of actin known to be induced by the treatment of cells with CD (32) (Fig. 3*B*). No internal toxin-containing vesicles were observed in CD-treated cells (Fig. 3*B*). Clearly, VacA was bound to the surface and surrounded the actin patches present on the cytoplasmic face of the plasma membrane (Fig. 3*C*). This localization of the toxin in CD-treated cells was confirmed at the ultrastructural level using immunogold labeling of VacA (Fig. 3*D*). Again, VacA molecules were localized around these "cauliflower-like" membrane protrusions induced by the CD treatment.

In a previous study (18), we observed, at the ultrastructural level by immunogold VacA labeling, an identical density of VacA molecules in endosomal/vacuolar area in PI-PLC-treated or untreated cells intoxicated with VacA. This indicates that VacA could be internalized in the absence of cell surface-associated GPI-Ps (18). Using the indirect immunofluorescence technique described for the CD treatment to observe VacA internalization, we found that the PI-PLC treatment of HeLa reduced VacA internalization (not shown).

Removal of GPI-Ps from the Cell Surface or Depolymerization of the Actin Cytoskeleton Does Not Affect VacA Localization in Lipid Rafts—We then investigated whether removing surface-associated GPI-Ps from HeLa cells by PI-PLC or CD modified the association of VacA with lipid rafts. Treatment of HeLa cells with PI-PLC was effective because it strongly reduced the CD55 immunoblot signal (CD55 being a GPI-P different from CD59, shown in Fig. 2*B*). Removal of GPI-Ps did not modify the association of VacA with lipid rafts (Fig. 4*A*). As shown in Fig. 4*B*, disruption of the HeLa cell cytoskeleton by CD also did not modify the association of VacA with lipid rafts (Fig. 4*B*). Quantitative evaluations of VacA in lipid rafts in PI-PLC- and CD-treated cells as well as in control preparations were performed. No significant differences in the amounts of VacA associated with lipid rafts were observed in PI-PLC- or CD-treated cells compared with control preparations (Fig. 4*C*).

Removal of GPI-Ps from HeLa Cell Surface, but Not Depolymerization of the Actin Cytoskeleton, Reduces Both the Influx

Downloaded from http://www.jbc.org/ by guest on July 27, 2018

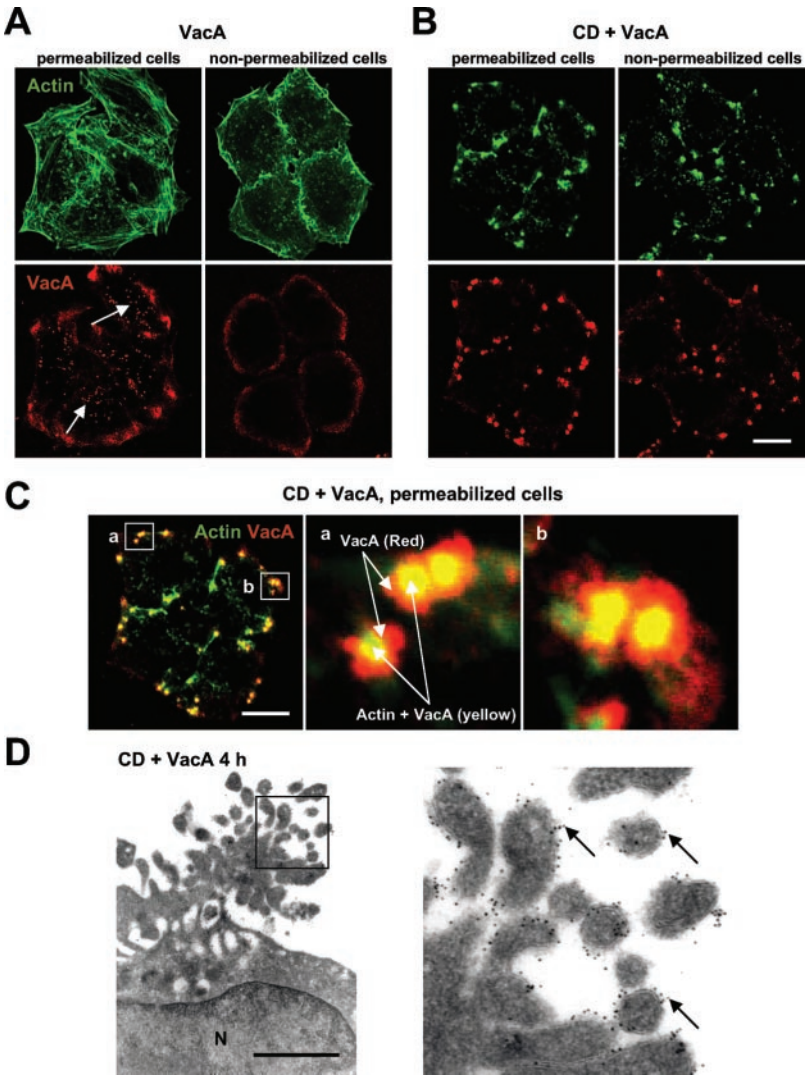

FIG. 3. **Disruption of HeLa cell cytoskeleton blocks VacA endocytosis.** *A*, control HeLa cells were incubated for 1 h at 4 °C with 2 μg/ml of VacA and then rinsed with medium at 4 °C to remove unbound toxin molecules. The cells were then warmed up by the addition of medium at 37 °C and incubated for 30 min at 37 °C. The preparations were then washed, permeabilized (*left panels*) or not (*right panels*) and processed for the detection of VacA by indirect fluorescence (*red fluorescence*) and actin staining (*green fluorescence*) (see "Experimental Procedures"). The *arrows* indicate intracellular vesicles containing VacA. *B*, HeLa cells were treated with CD (see "Experimental Procedures"), and the cells were then incubated with VacA (2 μg/ml) still in the presence of CD and processed for immunolocalization of the toxin as in *A*. *Left panels*, permeabilized cells; *right panels*, nonpermeabilized cells. *C*, merged images between actin (*green fluorescence*) and VacA (*red fluorescence*) bound to the surface of HeLa cells treated by CD and then by VacA (as in *B*). *Squares a* and *b* in the *left panel* delimit two fields of a cell, respectively, enlarged in *panels a* and *b* to the *right*. *D*, *left panel*, immunolocalization at the ultrastructural level, by immunogold labeling, of VacA bound on HeLa cells membrane protrusions induced by the CD treatment. *Right panel*, enlargement of the field delimited by the *square* in the *left panel*. The *arrows* indicate the positions of VacA decorated by gold particles. Scale bars, 10 μm for *A–C* and 1 μm for *D*.

and Efflux of Cl^- Induced by the VacA Channel—We then tested the chloride conductance of the VacA channel in cells depleted in GPI-Ps. HeLa cells treated with PI-PLC and incubated with or without 2 μg/ml of activated purified VacA were loaded with MEQ and then tested for chloride transport. As shown in Fig. 5*B*, removal of GPI-Ps from the HeLa cell surface reduced both the efflux (GM substitution) and influx (NM substitution) of chloride ions in cells compared with VacA untreated preparation (but incubated with cycloheximide as for PI-PLC treatment) (Fig. 5*A*). Quantification of the influx and the efflux of Cl^- through the VacA channel in cells treated or not by PI-PLC (or by cycloheximide alone, used in conjunction with PI-PLC to block the resynthesis of GPI-Ps (18)) is shown in Fig. 5*C*. Treatment of cells with PI-PLC reduced of about 50% both the influx and the efflux of Cl^- by the VacA channel (Fig. 5*C*). Cycloheximide alone did not interfere with the VacA channel activity (Fig. 5*C*).

Using the MEQ fluorescence assay, we then tested whether cell treatment with CD modified the VacA channel activity. As evidenced by Fig. 5*C*, treatment of cells with CD was found to increase both the influx and the efflux of chloride ions to about 40% in cells treated by VacA.

VacA Channel Allows Accumulation of Weak Base and Osmotic Swelling of Late Endosomes—It is well documented that acidic intracellular compartments such as lysosomes allow weak bases (such as NH_4Cl) to accumulate, provoking an osmotic swelling and resulting in vacuolation (33). In this respect, chloroquine has been described as the most efficient weak base in causing cell vacuolation of macrophage lysosomes (33). We therefore investigated whether a low concentration of chloroquine (1 mM) could mimic VacA-induced cell vacuolation. To this purpose, the cells were transfected either with GFP-Rab7 or GFP-Rab5 DNA to trace which type of intracellular compartments swelled under chloroquine treatment. The cells were then incubated with chloroquine alone or with VacA in the presence of 5 mM NH_4Cl. As shown in Fig. 6*A*, the chloroquine-induced vacuoles in HeLa cells were selectively decorated by Rab7 and were thus virtually identical to VacA-induced vacuoles (Fig. 6*A*). The kinetics of vacuole formation in HeLa cells by chloroquine alone (1 mM) or by this weak base at 1 mM in the presence of VacA are shown in Fig. 6*B*. Cell vacuolation onset in chloroquine- or VacA/chloroquine-treated cells was observed for 2 h after the addition of the weak base (Fig. 6*B*). Vacuoles induced by chloroquine alone at early time points were smaller than those induced by VacA plus chloroquine (Fig. 6*B*). The kinetics of vacuolation induced by chloroquine alone or VacA plus chloroquine are shown in the videos in the supplemental material. The addition of 20 μM NPPB to the culture medium efficiently blocked the formation of vacuoles induced by either chloroquine or VacA in the presence of 5 mM NH_4Cl (Fig. 6, *A* and *C*), indicating that both processes probably required Cl^- channels. To investigate whether the NPPB effects toward chloroquine-induced vacuoles and VacA-induced vacuoles might be similar, we studied the dose-re-

Downloaded from http://www.jbc.org/ by guest on July 27, 2018

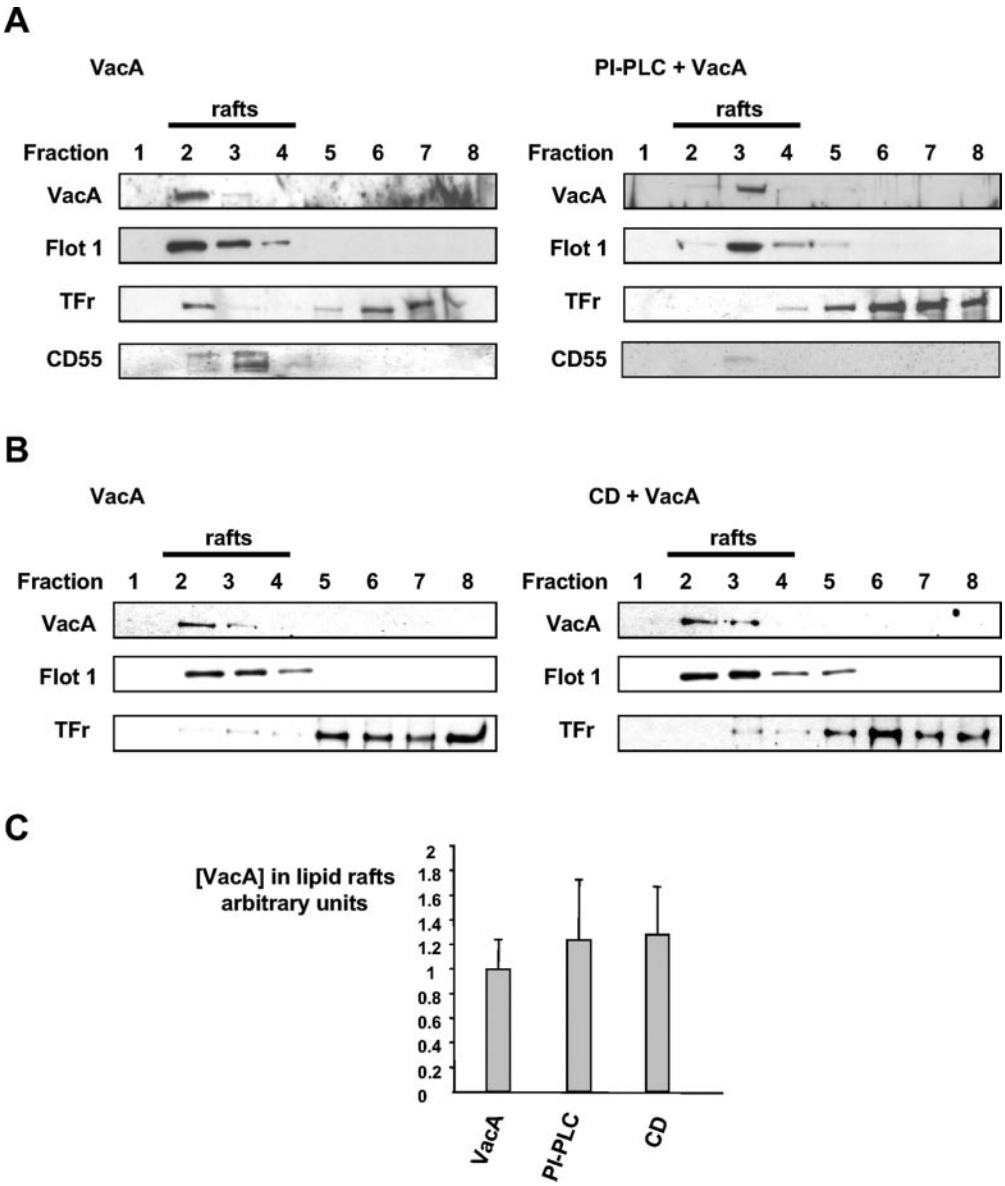

FIG. 4. **Removing GPI-Ps from HeLa cell surface or disrupting their actin cytoskeleton does not affect VacA localization in lipid rafts.** Density gradients for lipid rafts analysis (see "Experimental Procedures") of untreated or PI-PLC-treated cells (*A*) incubated with VacA untreated or CD-treated cells incubated with VacA (*B*). In *A* and *B*, HeLa cells were incubated with VacA (2 μg/ml) for 1 h at 4 °C, washed, warmed for 30 min at 37 °C, and lysed in 1% Triton X-100 at 4 °C. Identification of the proteins in each fraction was performed by immunoblot using the IgG 958 for VacA, the mAb anti-flotillin for flotillin 1 (*Flot 1*) (a marker of lipid rafts), and the mAb anti-transferrin receptor (*TFr*) (as a protein marker excluded from lipid rafts). Detection of CD55 by the mAb anti-CD55 was used to control the efficiency of the PI-PLC treatment. *C*, quantitative evaluation of VacA in lipid rafts. Anti-flotillin 1 immunoblots were used to normalize the VacA signals.

sponse relationship of NPPB-induced inhibition of vacuolation using the neutral red dye uptake assay. We found that NPPB exerted a concentration-dependent inhibition of vacuolation in cells treated with chloroquine alone or VacA (plus NH_4Cl) in a similar fashion, with a 50% inhibitory dose at 5 μM of NPPB in both experimental conditions (Fig. 6*C*). Finally, we have shown that NPPB was also effective in inhibiting the vacuolating effect of VacA in the presence of 0.1 mM chloroquine instead of NH_4Cl in the extracellular medium (Fig. 6*C*).

DISCUSSION

In the present work, we have shown that treatments of HeLa cells by PI-PLC (which removes specifically cell surface-associated GPI-Ps) and by CD (which leads to the disruption of the actin cytoskeleton) had opposite effects on the transport of chloride ions by VacA channels but converging effects on the toxin-induced vacuolation. Elimination of GPI-Ps from the cell surface strongly affected the VacA channel activity without interfering notably on the toxin endocytosis, whereas disruption of the actin cytoskeleton increased its overall chloride transport activity and strongly blocked VacA cell internalization. These data support the notion that the VacA pore is formed at the cell surface level and upon endocytosis provokes vacuolation.

That GPI-Ps are not required for VacA cell binding and localization in lipid rafts is in agreement with a recent report showing that, in CHO cells defective in GPI-Ps, VacA was localized in lipid rafts and still able to induce vacuolation (20). Moreover, our results also fit very well with the data of Kuo and Wang (17) showing that there was no difference in VacA binding between wild-type CHO cells, CHO cells treated with PI-PLC, or CHO cells overexpressing the fasI GPI-Ps. Therefore VacA, different from the pore-forming toxin aerolysin and related molecules (34), binds cells on lipid rafts but independently of the presence of GPI-Ps.

Downloaded from http://www.jbc.org/ by guest on July 27, 2018

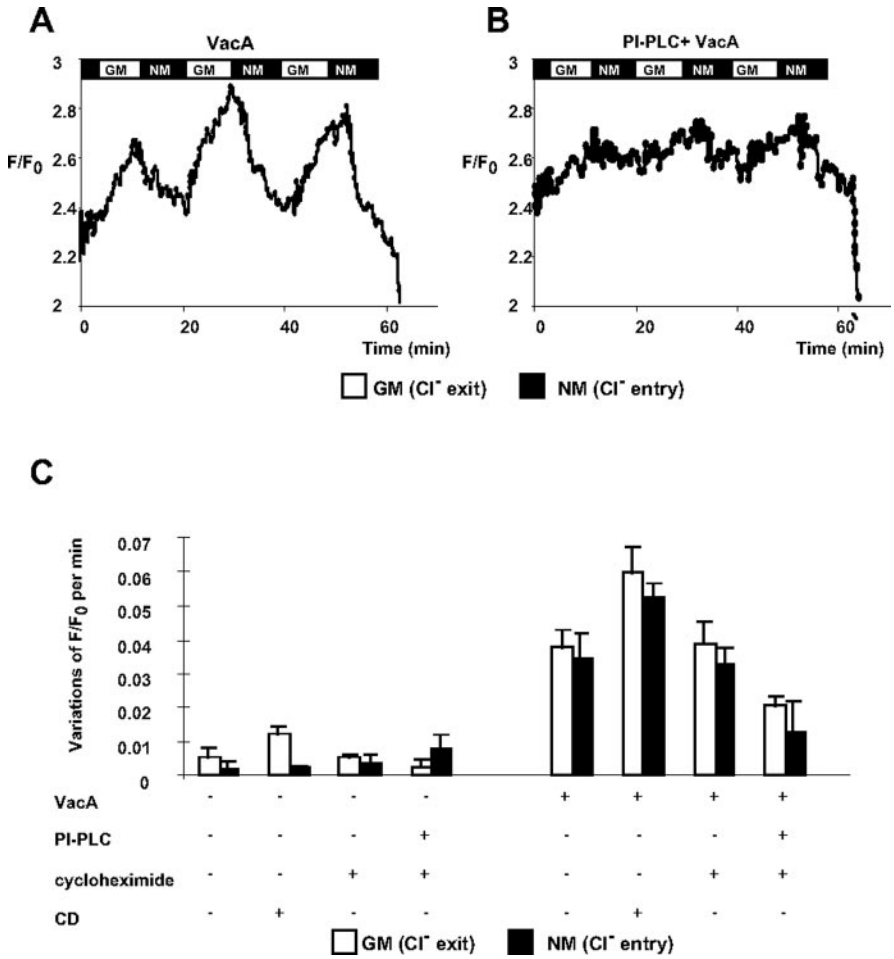

FIG. 5. **Removing GPI-Ps from HeLa cells surface inhibit both the influx and the efflux of Cl^- from cells induced by the VacA channel, but disruption of the actin cytoskeleton increased the cell overall transport of Cl^- by the toxin channel.** *A*, typical variation of MEQ F/F_0 obtained upon iterative GM followed by NM buffer substitutions of HeLa cells treated with cycloheximide and incubated with VacA (2 μg/ml) (average of MEQ fluorescence of 14 cells). *B*, variation of MEQ F/F_0 obtained upon iterative GM followed by NM buffer substitutions of HeLa cells treated with PI-PLC together with cycloheximide and incubated with VacA (2 μg/ml) as in *A* (average of MEQ fluorescence of 13 cells). *C*, histograms of variations of the relative MEQ fluorescence slopes (absolute values) during GM (white columns) or NM (black columns) substitutions. The cells were treated or not with PI-PLC or CD and then intoxicated or not with VacA (2 μg/ml) for 30 min (see "Experimental Procedures") before MEQ fluorescence recording. Each histogram represents an average of three independent experiments with a recording of MEQ fluorescence of 10–23 cells for each assay.

The presence of GPI-Ps on the cell surface, however, increases the VacA-induced vacuolation of cells (17, 18). It is now established that VacA does not use the clathrin-coated pit pathway of endocytosis but rather a caveolae-like internalization process requiring lipid rafts (18). GPI-Ps are components of lipid rafts (21, 22), and it has been shown recently that VacA may share a common endocytic pathway with GPI-Ps (17).

The mechanism by which VacA causes large Rab7-positive vacuoles may involve the transport of chloride ions by toxin channels (2, 11, 12, 35). This is likely because (i) the anion channel blocker NPPB inhibits VacA-induced vacuolation (11, 12, this study); (ii) it is well established that VacA-induced vacuolation requires the V-ATPase activity (2), and it has been recently documented that the rate-limiting step in late endosome acidification by the V-ATPase is the endosomal influx of chloride ions by specific channels that could be inhibited by NPPB (36, 37); and (iii) VacA mutant proteins, with an impaired capacity to form active channels, are unable (or poorly able) to vacuolate cells (38, 39). It is not clear, however, where the toxin channel is formed in the cell. On one hand it is hypothesized that the VacA channel might be formed at the level of the cell plasma membrane and then endocytosed into late endosome to provoke vacuolation (11, 12, 35). On the other hand, the demonstration that vacuolation could be observed in cells transfected with VacA DNA and expressing the toxin (13, 14) has pushed forward the idea that VacA, upon its translocation into the cytosol, could form channels into endomembranes such as those of late endosomes (2, 13, 14). This latter hypothesis was strengthened by the observation that expression into HeLa cells of a dominant negative mutant of VacA was able to antagonize the cell vacuolation induced by the wild-type toxin also expressed within the cytosol (39, 40). That removing GPI-Ps from the cell surface strongly reduced both the influx and efflux of chloride ions of the toxin pore and greatly affected the formation of large vacuoles in cells indicates that the VacA channel is formed at the level of the cell surface and responsible for the vacuolation as postulated (11, 12, 35).

Our results do not indicate whether the removal of GPI-Ps from the HeLa cell surface reduces the intrinsic chloride transport of the VacA channel or the formation of active toxin pores. The hydrophilic protein part of GPI-Ps may favor VacA insertion into lipid rafts. Alternatively, lipid rafts may be modified, as reported (41) when GPI-Ps are removed. This may alter the composition of detergent-resistant lipid-rich domains modifying for instance the capacity of VacA to form active channels. Also, subtle changes in the lipid composition of lipid rafts caused by GPI-Ps removal may affect the functionality of VacA channels (15).

Different from GPI-Ps removal, disruption of actin cytoskeleton of HeLa cells by CD increased the overall chloride transport activity by cells through VacA channels but inhibited large vacuoles formation (depolymerization of the actin cytoskeleton having been shown previously (18) to have no effect on the process of VacA vacuolation *per se*). These results eliminate the possibility that the VacA channel acts on cell vacuolation directly from the plasma membrane. Also, our observation that CD treatment strongly reduced the endocytosis of the toxin rules out the possibility that the VacA channel is formed in an intracellular compartment possibly under the influence of an acidic pH as reported in artificial bilayers (8) or in the cytosol (13, 14, 39, 40). The facts that CD treatment blocked VacA

Downloaded from http://www.jbc.org/ by guest on July 27, 2018

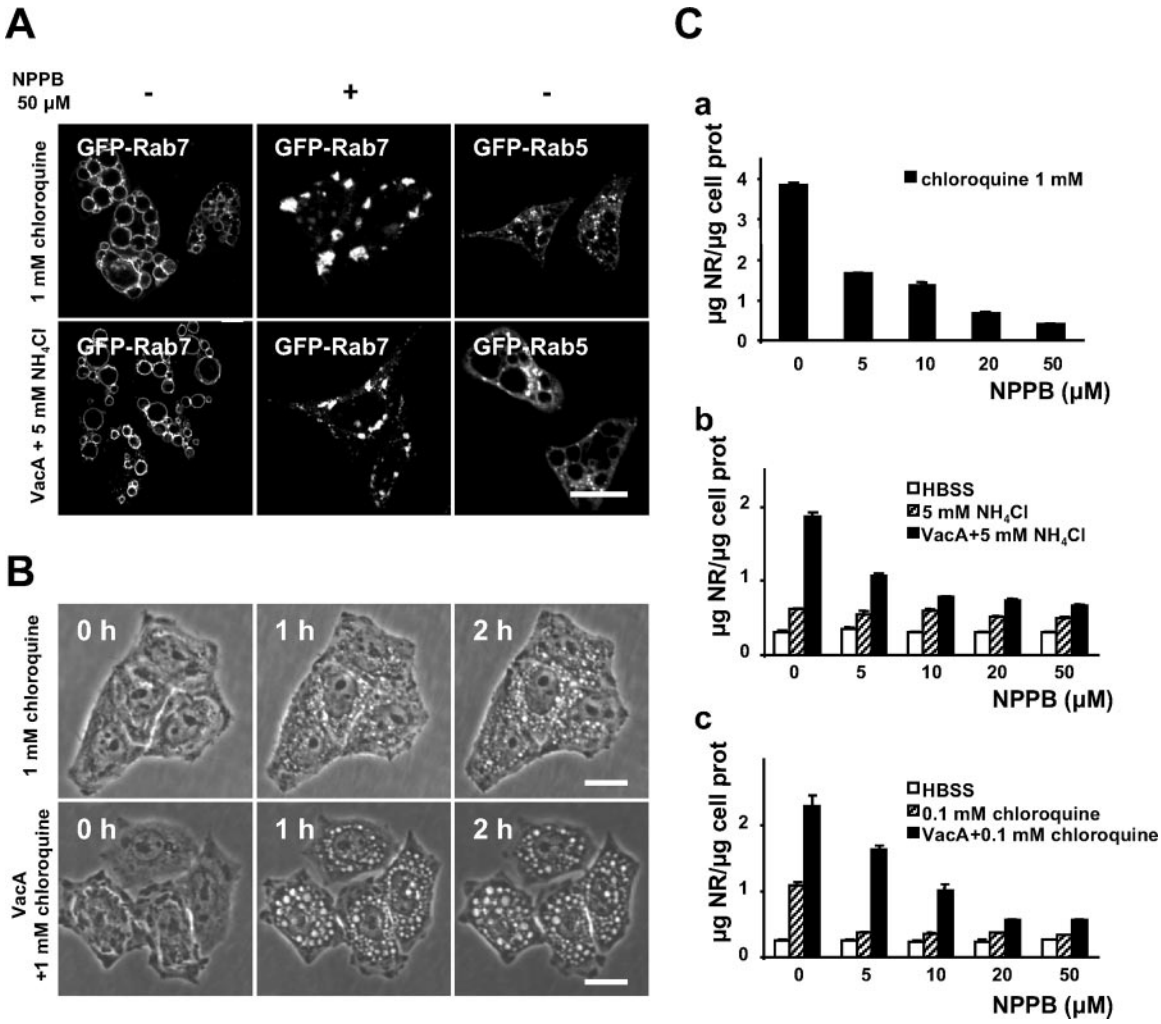

FIG. 6. **Chloroquine induces formation of large vacuoles specifically decorated by Rab7 that can be inhibited by the Cl^-channel blocker NPPB.** *A*, HeLa cells were transfected with plasmid vectors encoding either the GFP-labeled small GTPase Rab7 or Rab5. Upon proteins expression, the cells were intoxicated or not with 2 μg/ml of VacA for 30 min at 37 °C. Monolayers were then washed, and the cells not intoxicated with VacA were placed in HBSS containing 1 mM chloroquine, whereas those intoxicated with VacA were placed in HBSS containing 5 mM NH_4Cl and incubated at 37 °C for 5 h in the presence or not of 50 μM NPPB. After fixation, the cells were analyzed by confocal microscopy. *Scale bar*, 10 μm. *B*, kinetics of vacuole development in cells treated with 1 mM chloroquine alone for 2 h or preintoxicated with VacA (2 μg/ml) for 30 min at 37 °C and then incubated (after washing with HBSS) with 1 mM chloroquine for 2 h. (See also supplemental video 1 for chloroquine alone and supplemental video 2 for VacA plus chloroquine). *Scale bar*, 10 μm. *C*, neutral red dye uptake assays. *Panel a*, effects of NPPB on cell vacuolation induced by 1 mM chloroquine. The cells were incubated with HBSS containing 1 mM chloroquine for 5 h and increasing concentrations of NPPB. *Panel b*, effects of NPPB on VacA-induced cell vacuolation. The cells were intoxicated or not with 2 μg/ml of VacA for 30 min at 37 °C, and after washing the cells were placed in HBSS containing 5 mM NH_4Cl for 5 h. *Panel c*, effects of NPPB on VacA-induced cell vacuolation in the presence of chloroquine. The cells were intoxicated with 2 μg/ml of VacA for 30 min at 37 °C, and after washing the cells were incubated in HBSS containing 0.1 mM chloroquine for 5 h at 37 °C.

endocytosis, did not delocalize it from lipid rafts, increased the overall transport of toxin-dependent transport of chloride ions, and blocked vacuolation suggest that internalization of the toxin pore induces vacuolation.

We observed in HeLa cells with a disrupted actin cytoskeleton that VacA was clustered in protrusion-like structures induced by CD. It has been proposed that actin filaments, assembled at the tip of transmembrane proteins on the cytoplasmic side of the plasma membrane, compartmentalize lipid rafts and limit their mobility in a process called "pickets and fence" (42). When the actin cytoskeleton is not properly assembled, there is the possibility that large lipid rafts may thus be formed. This may explain our observation of toxin clustering in CD-treated cells without delocalization of VacA from lipid rafts. More importantly, inhibition of the toxin endocytosis by CD indicates that VacA relies on an actin-dependent process of internalization. Together with the observation that VacA binds to lipid rafts, it suggests that endocytosis of VacA utilizes a caveolae-like form of endocytosis (23). The observation that the overall transport of Cl^- by the VacA channel was increased in CD-treated cells could be mainly the consequence of the fact that, upon inhibition of VacA endocytosis, a higher number of VacA channels were maintained on the plasma membrane.

In the present study we have shown that cell vacuolation induced by the weak base chloroquine alone could (like VacA) induce the formation of large vacuoles, decorated specifically with Rab7, which could be blocked by NPPB. The anionic channel blocker NPPB has been reported, however, to decrease the activity of the nonselective calcium-activated cationic channel, but 100 μM NPPB was required in this study to reduce only to 50% the activity of this channel (43). We have shown in the present work that as low as 5 μM of NPPB was required to decrease 50% of the vacuolation of HeLa cells induced by 1 mM chloroquine and that the same concentration of NPPB totally prevented the vacuolation induced by 0.1 mM chloroquine (Fig. 6*C*). This indicates that chloride ions are probably specifically

Downloaded from http://www.jbc.org/ by guest on July 27, 2018

required for the cell vacuolation induced by chloroquine.

Two cellular activities of VacA, independent of vacuolation, have been recently described. In epithelial cells, VacA induces apoptosis by provoking the release of cytochrome *c* from mitochondria (1). In T-lymphocytes VacA blocks the nuclear translocation of the transcription factor NFAT in a similar fashion as immunosuppressive agents such as cyclosporin A or FK506 (44). Both activities apparently require the ability of the toxin to induce vacuolation (1, 44). Induction of cytochrome *c* leakage and inhibition of NFAT nuclear translocation both necessitate probably the translocation of VacA (or part of it) into the cytosol (1, 44). With the notion that the VacA pore is formed at the level of the plasma membrane and is endocytosed to provoke the osmotic swelling of late endosomes, we propose that this mechanism might be used in fact by the toxin to gain access to the cytosol. Through the rupture of overswelled vacuoles, VacA might indeed be released in the cytosol and could reach one (or several) intracellular target(s).

Acknowledgments—We thank Dr. T. L. Cover (Vanderbilt University) for the generous gifts of the anti-VacA rabbit IgG 958 and HeLa cells. We also acknowledge Drs. M. Gauthier and E. Lemichez (INSERM U452, Nice, France) for critical reading of the manuscript, Dr. M. Bidet (CNRS UMR 65–48, Faculté des Sciences, Parc Valrose, Nice, France) for advice during MEQ fluorescence experiments, P. Monzo (INSERM U568, Nice, France) for continuous help during this work, B. Mesmin (Faculté des Sciences, Parc Valrose, Nice, France) for technical assistance, and Y. Le Marchand-Brustel and the Bettencourt-Schueller's foundation for video microscopy facilities.

REFERENCES

1. Boquet, P., Ricci, V., Galmiche, A., and Gauthier, N. C. (2003) *Trends Microbiol.* **11,** 410–413
2. Papini, E., Zoratti, M., and Cover, T. L. (2001) *Toxicon* **39,** 1757–1767
3. Salama, N. R., Otto, G., Tompkins, L., and Falkow, S. (2001) *Infect. Immun.* **69,** 730–736
4. Cover, T. L. (1996) *Mol. Microbiol.* **20,** 241–246
5. Cover, T. L., Hanson, P. I., and Heuser, J. E. (1997) *J. Cell Biol.* **138,** 759–769
6. Lupetti, P., Heuser, J. E., Manetti, R., Massari, P., Lanzavecchia, S., Bellon, P. L., Dallai, R., Rappuoli, R., and Telford, J. L. (1996) *J. Cell Biol.* **133,** 801–807
7. Papini, E., de Bernard, M., Milia, E., Bugnoli, M., Zerial, M., Rappuoli, R., and Montecucco, C. (1994) *Proc. Natl. Acad. Sci. U. S. A.* **91,** 9720–9724
8. Czajkowsky, D. M., Iwamoto, H., Cover, T. L., and Shao, Z. (1999) *Proc. Natl. Acad. Sci. U. S. A.* **96,** 2001–2006
9. Tombola, F., Carlesso, C., Szabò, I., de Bernard, M., Reyrat, J. M., Telford, J. L., Rappuoli, R., Montecucco, C., and Zoratti, M. (1999) *Biochem. J.* **76,** 1401–1419
10. Iwamoto, H., Czajkowsky, D. M., Cover, T. L., Szabo, G., and Shao, Z. (1999) *FEBS Lett.* **450,** 101–104
11. Tombola, F., Oregna, F., Brutsche, S., Szabò, I., Del Giudice, G., Rappuoli, R., Montecucco, C., Papini, E., and Zoratti, M. (1999) *FEBS Lett.* **460,** 221–225
12. Szabò, I., Brutsche, S., Tombola, F., Moschioni, M., Satin, B., Telford, J. L., Rappuoli, R., Montecucco, C., Papini, E., and Zoratti, M. (1999) *EMBO J.* **18,** 5517–5527
13. de Bernard, M., Arico, B., Papini, E., Rizzuto, R., Grandi, G., Rappuoli, R., and Montecucco, C. (1997) *Mol. Microbiol.* **26,** 665–674
14. Ye, D., Willhite, D. C., and Blanke, S. R. (1999) *J. Biol. Chem.* **274,** 9277–9282
15. Adrian, M., Cover, T. L., Dubochet, J., and Heuser, J. E. (2002) *J. Mol. Biol.* **318,** 121–133
16. Garner, J. A., and Cover, T. L. (1996) *Infect. Immun.* **64,** 4197–4203
17. Kuo, C. H., and Wang, W. C. (2003) *Biochem. Biophys. Res. Comm.* **303,** 640–644
18. Ricci V., Galmiche, A., Doye, A., Necchi, V., Solcia, E., and Boquet, P. (2000) *Mol. Biol. Cell* **11,** 3897–3909
19. Cross, G. A. (1990) *Annu. Rev. Cell Biol.* **6,** 1–39
20. Schraw, W., Li, Y., McClain, M. S., van der Goot, F. G., and Cover, T. L. (2002) *J. Biol. Chem.* **277,** 34642–34650
21. Simons, K., and Ikonen, E. (1997) *Nature* **387,** 569–572
22. Varma, R., and Mayor, S. (1998) *Nature* **394,** 798–801
23. Nichols, B. J., and Lippincott-Schwartz, J. (2001) *Trends Cell Biol.* **11,** 406–412
24. Patel, H. K., Willhite, D. C., Patel, R. M., Ye, D., Williams, C. L., Torres, E. M., Marty, K. B., MacDonald, R. A., and Blanke, S. (2002) *Infect. Immun.* **70,** 4120–4123
25. Hotchin, N. A., Cover, T. L., and Aktar, N. (2000) *J. Biol. Chem.* **275,** 14009–14012
26. Cover, T. L., and Blaser, M. J. (1997) *J. Biol. Chem.* **267,** 10570–10575
27. de Bernard, M., Papini, E., de Filippis, V., Gottardi, E., Telford, J., Manetti, R., Fontana, A., Rappuoli, R., and Montecucco, C. (1995) *J. Biol. Chem.* **270,** 23937–23940
28. Davitz, M. A., Low, M. G., and Nussenzweig, V. (1986) *J. Exp. Med.* **163,** 1150–1161
29. Deckert, M., Ticchioni, M., and Bernard, A. (1996) *J. Cell Biol.* **133,** 791–799
30. Ricci, V., Sommi, P., Fiocca, R., Romano, M., Solcia, E., and Ventura, U. (1997) *J. Pathol.* **183,** 453–459
31. Biwersi, J., and Verkman, A. S. (1991) *Biochemistry* **30,** 7879–7883
32. Peterson, J. R., and Mitchison, T. J. (2002) *Chem. Biol.* **9,** 1275–1285
33. Ohkuma, S., and Poole, B. (1981) *J. Cell Biol.* **90,** 656–664
34. Fivaz M., Abrami, L., Tsitrin, Y., and van der Goot, F. G. (2001) *Curr. Top. Microbiol. Immunol.* **257,** 35–52
35. Morbiato, L., Tombola, F., Campello, S., Del Giudice, G., Rappuoli, R., Zoratti, M., and Papini, E. (2001) *FEBS Lett.* **508,** 479–483
36. Sonawane, N. D. Thiagarajah, J. R., and Verkman, A. S. (2002) *J. Biol. Chem.* **277,** 5506–5513
37. Sonawane, N. D., and Verkman, A. S. (2003) *J. Cell Biol.* **160,** 1129–1138
38. Mclain M. S., Iwamoto, H., Cao, P., Vinion-Dubiel, A. D., Li, Y., Szabo, G., Shao, Z., and Cover, T. L. (2003) *J. Biol. Chem.* **278,** 12101–12108
39. Vinion-Dubiel, A. D., McClain, M., Czajkowsky, D. M., Iwamoto, H., Ye, D., Cao, P., Schraw, W., Szabo, G., Blanke, S. R., Shao, Z., and Cover, T. L. (1999) *J. Biol. Chem.* **274,** 37736–37742
40. Willhite, D. C., Ye, D., and Blanke, S. R. (2002) *Infect. Immun.* **70,** 3824–3832
41. Anderson, R. G. W., and Jacobson, K. (2002) *Science* **296,** 1821–1825
42. Fujiwara, T., Ritchie, K., Murakoshi, H., Jacobson, K., and Kusumi, A. (2002) *J. Cell Biol.* **157,** 1071–1081
43. Gogelein H., and Pfannmuller, B. (1989) *Pfluegers Arch. Eur. J. Physiol.* **41,** 287–298
44. Gebert, B., Fisher, W., Weiss, E., Hoffmann, R., and Haas, R. (2003) *Science* **301,** 1099–1102

Downloaded from http://www.jbc.org/ by guest on July 27, 2018

Glycosylphosphatidylinositol-anchored Proteins and Actin Cytoskeleton Modulate Chloride Transport by Channels Formed by the *Helicobacter pylori* Vacuolating Cytotoxin VacA in HeLa Cells

Nils C. Gauthier, Vittorio Ricci, Pierre Gounon, Anne Doye, Michel Tauc, Philippe Poujeol and Patrice Boquet

J. Biol. Chem. 2004, 279:9481-9489.
doi: 10.1074/jbc.M312040200 originally published online December 14, 2003

Access the most updated version of this article at doi: 10.1074/jbc.M312040200

Alerts:
- When this article is cited
- When a correction for this article is posted

Click here to choose from all of JBC's e-mail alerts

Supplemental material:
http://www.jbc.org/content/suppl/2004/01/22/M312040200.DC1

This article cites 44 references, 23 of which can be accessed free at
http://www.jbc.org/content/279/10/9481.full.html#ref-list-1

Downloaded from http://www.jbc.org/ by guest on July 27, 2018